Detection of High-Speed Voltage Waveforms in GaN Devices Using Electric-Field-Induced Second-Harmonic Generation

Daniel J. Kane and William Wood

Abstract—**We use electric-field-induced second-harmonic generation (EFISHG) to measure high-speed voltage waveforms in commercial GaN light-emitting diodes (LEDs). The output of an ultrafast passively mode-locked Ti : sapphire laser is reflected from the surface of a GaN UV LED. Copropagating with the specularly reflected Ti : sapphire fundamental is second-harmonic light that is proportional to and synchronous with a high-speed voltage pulse that reverse biases the LED. The measured amplitude of the detected pulse was found to vary with dc bias across the p-n junction of the LED indicating that the detected voltage waveform was localized to the p-n junction. Because of synchronous detection, the detection bandwidth (<10 THz) is limited only by the pulsewidth of the probe laser pulse (<100 fs).**

Index Terms— **Gallium compounds, nonlinear optics, p-n junctions, signal sampling, ultrafast electronics, ultrafast optics.**

I. Introduction

EVALUATION of fast semiconductor devices requires both high temporal resolution and the ability to probe internal points of the device under test (DUT) noninvasively. While optical methods are suitable for this application, centrosymmetric semiconductors such as silicon and germanium usually require an external electrooptic probe placed within the fringe electric field flux lines of the region of interest, reducing sensitivity, adding parasitic capacitance to the probed circuit, and limiting the ability to probe internal devices. However, past work has shown that second-harmonic generation via the third-order susceptibility can occur in semiconductors when an electric field within the semiconductor breaks the symmetry that prevents second-harmonic generation from occurring [1]–[10].

While voltages in semiconductors are quite small, because the voltage drop occurs only over a very narrow depletion region within the p-n junction, electric fields can surpass 10^6 V/cm. When these large electric fields interact with an external probe laser via the $\chi^{(3)}$ of the semiconductor, the second harmonic of the probe laser ($P \propto \cdot\chi^{(3)} E_{\mathrm{DC}} E^2_{\mathrm{probe}}$) is produced. This process is known as electric-field-induced second-harmonic generation (EFISHG or sometimes EFISH).

EFISHG has been observed at metal–semiconductor (silicon) junctions [1], semiconductor–insulator (Si–SiO_2) interfaces [2], [3], in GaAs–AlGaAs quantum wells [4], in capacitors [5], as well as organic light-emitting diodes (LEDs) [6]. It has also been used to measure wave propagation in silicon waveguides [7]. However, in all of these studies, the probe laser was above the bandgap of silicon (800 nm–1 μm) producing large carrier concentrations and electron plasmas [8], [9]. Such plasmas can produce localized metallic behavior, greatly increasing the conductivity where the laser pulse interacts with the semiconductor. Thus, the local electric field can become effectively zero, quenching the EFISHG signal and perturbing the measurement. Worse, injected photocurrent into the p-n junction could also affect the measurement.

In previous work, using low-speed asynchronous detection, we showed that it was possible to noninvasively monitor low frequency voltage waveforms in a GaN photodiodes using EFISHG by using wavelengths such that both the fundamental and the second harmonic are below the bandgap of the semiconductor [10]. Unfortunately, the detection bandwidth of our previous work was limited ($\ll$1 MHz) by the fact that the voltage waveforms in the DUT were not synchronized with the laser pulses. As a result, the detection bandwidth was limited by the time response of the detector. In this letter, we extend our previous work by synchronizing the voltage pulses in the device with the laser probe pulses allowing the detection bandwidth to be limited by only the probe laser pulsewidth (<100 fs, detection bandwidth <10 THz) while preserving the ability to average scans to improve the signal-to-noise ratio. In addition, by incorporating an electronic time delay, we were able to utilize an efficient differential detection scheme to remove the considerable background caused by bulk contributions.

II. Experiment

Fig. 1 is a schematic diagram of the apparatus used for the waveform measurements. The probe laser beam of ~100-fs pulses is generated by a passively mode-locked Ti : sapphire laser set to approximately 806 nm to insure both the fundamental and second harmonic are below the bandgap of the probed material, reducing induced photocurrents. The probe is focused onto a semiconductor device (in this case, a commercial UV LED) to a spot size of ~20 μm. A half-wave plate and polarizer are used for variable attenuation and polarization control of the probe beam. A beam splitter sends a portion of the beam to a photodiode to monitor the mode-locked laser and synchronize the detection electronics (see below). The probe beam is incident at ~45° to the sample surface. The SHG signal copropagates with the specular probe beam and is directed though a 1/8-m spectrometer. UV pass/visible blocking filters are used in front of the spectrometer to block any residual fundamental before reaching the 1P28 photomultiplier tube (PMT).

Manuscript received January 4, 2006; revised April 4, 2006. This material is based upon work supported by the National Science Foundation under Grant DMI-0091454.

D. J. Kane is with Southwest Sciences, Inc., Santa Fe, NM 87505 USA (e-mail: djkane@swsciences.com).

W. Wood is with WWood Consulting, LLC, Mount Calvary, WI 53057 USA.

Digital Object Identifier 10.1109/LPT.2006.879920

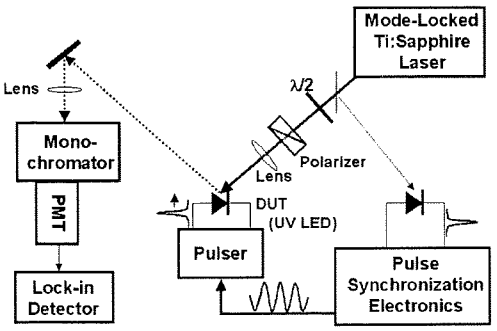

Fig. 1. Schematic diagram of the EFISHG probe using reflection geometry. The probe beam is reflected from the surface of the UV LED DUT. The signal copropogates with the probe beam. The signal is separated from the probe using a spectrometer.

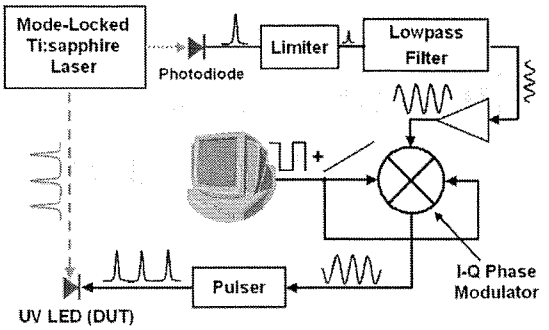

Fig. 2. Schematic diagram of the detection electronics for the EFISHG probe depicts the electronics used for pulse synchronization. The laser pulse train is monitored using a photodiode. The output from the photodiode is amplified, limited, and filtered before being sent into a microwave phase shifter. A computer calculates the sine and cosine values for a dither and ramp that phase shift the input sine wave. The output sine wave is used to trigger a pulse generator connected to the DUT.

The voltage-induced EFISHG signal was found to be linear in applied voltage. In general, we expect the EFISHG signal to be quadratic in applied voltage because

$$I_{2\omega} \propto P_{2\omega}^2 \propto |\chi^{(3)} E_\omega^2 E_v|^2 \tag{1}$$

where $\chi^{(3)}$ is the third-order nonlinear susceptibility, $P_{2\omega}$ is the second-harmonic polarization, E_ω is the electric field due to the laser pulse, and E_v is the electric field due to the applied voltage. However, there is a background polarization from second-harmonic generation by the bulk GaN, by surface interaction, and by EFISHG via a piezoelectric field caused by strain in the GaN lattice [11]. If this polarization is denoted P_B, and the polarization due to the applied electric field is P_v, then the second-harmonic intensity is given by

$$I_{2\omega} \propto |P_v + P_B|^2 = |P_v|^2 + |P_B|^2 + 2\mathrm{Re}(P_v P_B^*) \tag{2}$$

where Re is the real part. If $P_B \gg P_v$, then homodyne detection becomes possible through the $2\mathrm{Re}(P_v P_B^*)$ term. Because P_v is proportional to E_v (1), the observed change in the second-harmonic signal is linear with respect to applied voltage. It should also be noted that the amount of heterodyning is dependent on the phase difference between P_v and P_B, which can cause the magnitude of the signal to change when probing different sections of the same device (i.e., speckle).

A bias tee (modified Avtech AVS-S1 for reverse bias applications) was used to isolate the dc bias on the LED from the high-frequency pulse applied to the LED. The electronic pulses (~200-ps full-width at half-maximum (FWHM) and 3-V peak amplitude) to the UV LED and the ultrashort laser pulses (<100 fs) from the mode-locked Ti : sapphire laser are synchronized and time delayed by phase modulating the sine wave trigger to the pulse generator (Avtech Model AVN-1-C). A microscope above the sample is used to visualize the alignment of the probe beam on the LED.

A pulsing circuit depicted in Fig. 2 synchronizes the mode-locked Ti : sapphire laser pulses with the voltage pulse. A small portion of the mode-locked Ti : sapphire is sent into an optical delay line, providing a coarse time delay, before being monitored by a high-speed silicon photodiode. The output from the photodiode is sent into a limiter before being filtered and amplified to produce an 88 MHz sine wave trigger for the pulse generator that is phase-locked to the mode-locked Ti : sapphire laser. This 88-MHz sine wave trigger is amplified and sent into an I and Q phase modulator to allow the relative phase, and hence delay, between the 88-MHz sine wave and the laser pulses to be adjusted.

The phase, or time delay, of the 88-MHz sine wave trigger is both scanned slowly, under computer control, to map out the entire waveform, and dithered to provide an efficient means for differential measurement. The slow scan of the phase controls the time delay ranging over 11.3 ns. The dither is set to delay the voltage pulse relative to the probe pulse by one-half the time separation of the probe pulses (5.7 ns) and runs at the lock-in frequency. Thus, signals separated by 5.7 ns are subtracted from each other, which removes the bulk contribution from the signal of interest. The output from the 1P28 PMT is sent to a lock-in amplifier that is phase-locked to the phase dither. Slowly ramping the phase yields a pulse (Fig. 3) clearly showing that the 200-ps input pulses are broadened to over 1.5 ns in the device due to the device impedance.

III. Results

Fig. 3(a) shows the comparison between a single scan and an average of ten scans. Each scan takes approximately 7.5 s to complete. Fig. 3(b) shows a comparison between different filter windows. There are approximately 5000 points in each scan, or about 1000 points/ns. The time constant of the lock-in amplifier was set to 100 ms, which effectively convolved a 67-point window with the measured signal, yielding an effective detection bandwidth of approximately 15 Gz. The ultimate detection bandwidth is determined by the probe laser's pulsewidth; higher bandwidths can be achieved by reducing the number of points in the scan and averaging. Shown for comparison in Fig. 3(b) is a pulse measured with the time constant of the lock-in amplifier set to 30 ms (~20-point window), which gives a detection bandwidth of about 50 GHz. In spite of the improved bandwidth, the overall measured pulse shape is changed very little.

In previous work, we determined the peak-induced photocurrent to be approximately 12 μA [10]. Assuming a 1-V peak voltage across the p-n junction of the GaN LED and a 15-GHz measurement bandwidth, the effective capacitance is 800 atto-Farads.

The noise level was determined by taking the average root-mean-square (rms) difference between the two plots shown in Fig. 3(a). Assuming a 1-V peak amplitude (the 3-V, 200-ps input

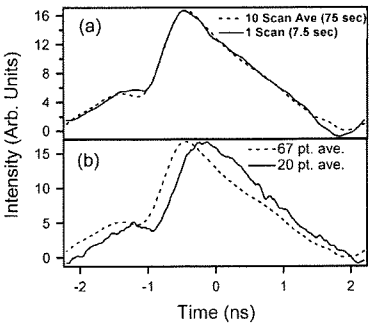

Fig. 3. (a) Comparison of a single scan of the pulse with (b) an average of ten scans. From this, together with the scan time and the time constant setting of the lock-in amplifier, we determine that the noise level is approximately 8.5 mV/Hz$^{-1/2}$.

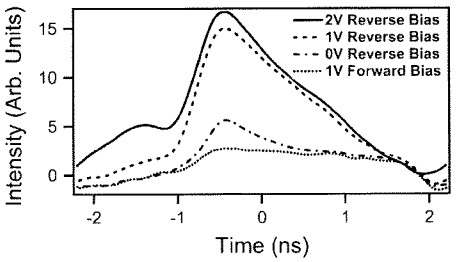

Fig. 4. Change in the measured waveform as a function of bias voltage. As the reverse bias voltage is reduced, the total capacitance of the p-n junction increases, lowering the voltage drop across the p-n junction. This, in turn, reduces the measured electric field.

pulse was broadened considerably), the noise was found to be approximately 27 mV in a 10-Hz window, or about 8.5 mV/Hz $^{-1/2}$, which is the rms noise for one time point if measured for 1 s. Thus, a 100-point waveform with a time spacing of 100 fs could be obtained in 10 s if an rms noise level of ~27 mV was acceptable – 100 s if a noise level of ~8.5-mV rms was desired.

Under forward bias, diffusion capacitance increases the effective capacitance of a p-n junction. Assuming the junction impendence is given by $|1/C\omega|$, where C is the total capacitance and ω is the frequency in radians/second, for a given frequency, the voltage drop and the electric field across the junction is inversely proportional to the capacitance. Thus, for a fixed pulsewidth, the observed EFISHG signal will be inversely proportional to the total capacitance of the p-n junction. To verify this, Fig. 4 shows the electronic pulse measured (~3-V peak, 200-ps FWHM input, broadened to 1.5 ns) across the p-n junction as a function of junction bias voltage (dc). Each plot is an average of ten scans, and the lock-in amplifier was set to have a time constant of 100 ms. A 2-V reverse bias causes a small junction capacitance, which produces the largest observed peak signal. As the junction becomes more forward biased, the capacitance in the p-n junction increases, reducing the impendence of the junction. As a result, the voltage drop of the high-speed pulse (< 1 ns) across the p-n junction decreases, decreasing the measured EFISHG signal. Once the junction is forward biased, the capacitance becomes high enough to reduce the voltage drop across the junction to such a low value that the EFISHG signal is barely observed. This also demonstrates that the measured EFISHG signal is specific to the voltage drop across the p-n junction. The origin of the shoulder that starts to appear at a reverse bias of 1 V is not known. However, because the signal is found by subtracting two points separated by 5.7 ns (one-half the time spacing between two probe pulses), it could be caused by extended ringing that is aliased into the detection window.

IV. Conclusion

We have demonstrated EFISHG for the measurement of high-speed voltage waveforms in commercial GaN devices. By electronically phase-locking the measured pulse to the mode-locked laser, the technique has reasonable signal-to-noise and can measure high-speed waveforms in a few seconds. The SHG signal is affected by the junction capacitance, which demonstrates that it emanates from the p-n junction itself. By keeping the second-harmonic photon energy below the bandgap of the semiconductor material being probed, induced currents are minimized, reducing the intrusiveness of the technique. Thus, EFISHG could be a useful tool for the *in situ* measurement of device parameters. However, even though our technique is limited in detection bandwidth by the pulsewidth of the probe pulse, device and circuit impedance still limit the bandwidth of the detected waveform.

References

[1] G. Lüpke, C. Meyer, C. Ohlhoff, H. Kurz, S. Lehmann, and G. Marowsky, "Optical second harmonic generation as a probe of electric-field-induced perturbation of centrosymetric media," *Opt. Lett.*, vol. 20, pp. 1997–1999, 1995.

[2] P. T. Wilson, Y. Jiang, O. A. Aktsipetrov, E. D. Mishina, and M. C. Downer, "Frequency-domain interferometric second-harmonic spectroscopy," *Opt. Lett.*, vol. 24, pp. 496–498, 1999.

[3] O. A. Aktsipetrov, A. A. Fedyanin, A. V. Melnikov, E. D. Mirshina, A. N. Rubtsov, M. H. Anderson, P. T. Wilson, M. ter Beek, X. F. Hu, J. I. Dadap, and M. C. Downer, "DC-electric-field-induced and low-frequency electromodulation second-harmonic generation spectroscopy of Si(001)-SiO_2 intefaces," *Phys. Rev. B*, vol. 60, pp. 8924–8938, 1999.

[4] A. Fiore, E. Rosencher, V. Berger, and J. Nagle, "Electric field induced interband second harmonic generation in GaAs/AlGaAs quantum wells," *Appl. Phys. Lett.*, vol. 67, pp. 3765–3767, 1995.

[5] T. V. Dologova, A. A. Fedyanin, and O. A. Aktsipetrov, "DC-electric-field-induced second-harmonic interferometry of the Si(111)-SiO_2 interface in Cr–SiO_2–Si MOS capacitor," *Phys. Rev. B*, vol. 68, p. 073307, 2003.

[6] R. Hildebrandt, H.-M. Keller, G. Marowsky, W. Brütting, T. Fehn, M. Schwoerer, and J. E. Sipe, "Electric-field-induced optical second harmonic generation in poly(phenylene vinylene) light emitting diodes," *Chem. Phys.*, vol. 245, pp. 341–344, 1999.

[7] A. Nahata, T. F. Heinz, and J. A. Misewich, "High-speed electrical sampling using optical second harmonic generation," *Appl. Phys. Lett.*, vol. 69, pp. 746–748, 1996.

[8] V. L. Malevich, "Dynamics of photoinduced field screening; THz-pulse and second harmonic generation from semiconductor surface," *Surface Sci.*, vol. 454-456, pp. 1074–1078, 2000.

[9] J. Dadap, P. T. Wilson, M. H. Anderson, M. C. Downer, and M. ter Beek, "Femtosecond carrier-induced screening of dc electric-field-induced second-harmonic generation at the Si(001)-SiO_2 interface," *Opt. Lett.*, vol. 22, pp. 901–903, 1997.

[10] K. A. Peterson and D. J. Kane, "Electric-field-induced second-harmonic generation in GaN devices," *Opt. Lett.*, vol. 26, pp. 438–440, 2001.

[11] C.-K. Sun, S.-W. Chu, S.-P. Tai, S. Keller, A. Abore, U. K. Mishra, and S. P. DenBaars, "Mapping piezoelectric filed distribution in gallium nitride with scanning second-harmonic generation microscopy," *Scanning*, vol. 23, p. 182, 2001.